JOURNAL OF BACTERIOLOGY, Oct. 2004, p. 6689–6697 Vol. 186, No. 20
0021-9193/04/$08.00+0 DOI: 10.1128/JB.186.20.6689–6697.2004

MicC, a Second Small-RNA Regulator of Omp Protein Expression in *Escherichia coli*

Shuo Chen,[1]† Aixia Zhang,[2]† Lawrence B. Blyn,[1] and Gisela Storz[2]*

IBIS Therapeutics, ISIS Pharmaceuticals, Inc., Carlsbad, California,[1] and Cell Biology and Metabolism Branch, National Institute of Child Health and Human Development, National Institutes of Health, Bethesda, Maryland[2]

Received 16 January 2004/Accepted 9 June 2004

In a previous bioinformatics-based search for novel small-RNA genes encoded by the *Escherichia coli* genome, we identified a region, IS063, located between the *ompN* and *ydbK* genes, that encodes an ~100-nucleotide small-RNA transcript. Here we show that the expression of this small RNA is increased at a low temperature and in minimal medium. Twenty-two nucleotides at the 5′ end of this transcript have the potential to form base pairs with the leader sequence of the mRNA encoding the outer membrane protein OmpC. The deletion of IS063 increased the expression of an *ompC-luc* translational fusion 1.5- to 2-fold, and a 10-fold overexpression of the small RNA led to a 2- to 3-fold repression of the fusion. Deletion and overexpression of the IS063 RNA also resulted in increases and decreases, respectively, in OmpC protein levels. Taken together, these results suggest that IS*063* is a regulator of OmpC expression; thus, the small RNA has been renamed MicC. The antisense regulation was further demonstrated by the finding that *micC* mutations were suppressed by compensatory mutations in the *ompC* mRNA. MicC was also shown to inhibit ribosome binding to the *ompC* mRNA leader in vitro and to require the Hfq RNA chaperone for its function. We suggest that the MicF and MicC RNAs act in conjunction with the EnvZ-OmpR two-component system to control the OmpF/OmpC protein ratio in response to a variety of environmental stimuli.

A burgeoning number of small RNAs have been identified in *Escherichia coli* over the past few years (4, 7, 21, 29, 33, 36). Some of these noncoding RNAs have been shown to act by forming base pairs with target sequences, while others bind specific proteins or have structural roles. However, the challenge remains to elucidate the functions of the vast majority of these RNAs.

Among the *E. coli* small RNAs, the most information is known about those that act as antisense riboregulators (reviewed in references 14, 31, 32, and 34). These RNAs exert their functions by forming base pairs with mRNAs that are generally encoded at separate loci. The net effect can be the up-regulation or down-regulation of target genes. Examples of small RNAs that block ribosome accessibility to target mRNAs and thereby decrease gene expression are MicF, which forms base pairs with the *ompF* mRNA; DicF, which forms base pairs with the *ftsZ* mRNA; OxyS, which forms base pairs with the *fhlA* mRNA; and Spot42, which forms base pairs with the *galETKM* mRNA. The DsrA and RprA small RNAs form base pairs with the *rpoS* mRNA and increase translation by preventing the formation of an inhibitory mRNA secondary structure. The formation of base pairs between the newly identified RyhB small RNA and its targets leads to the degradation of these mRNAs.

The MicF small RNA is encoded divergently from the gene encoding the OmpC porin and represses the expression of OmpF, another porin (1, 3, 15, 16). While their outer membranes prevent the passage of most molecules, *E. coli* cells possess three trimeric outer membrane porins, OmpC, OmpF, and PhoE, that allow fairly nonspecific passage of low-molecular-weight soluble molecules (reviewed in references 11 and 18). The *ompN* gene of *E. coli* encodes a homolog of the trimeric porins, but the OmpN protein has not yet been detected (20). The OmpC and OmpF porins are among the most abundant outer membrane proteins, and their expression is extensively regulated (reviewed in reference 19). OmpC, which has the smaller pore diameter of the two, is thought to be important in environments where nutrient and toxin concentrations are high, such as in the intestine, and it is the predominant porin at high temperatures and high osmolarities. OmpF, which has a larger pore diameter, is thought to be important in environments where nutrient and toxin concentrations are low, such as in fresh water, and it is more abundant at low temperatures and low osmolarities. Part of the differential response to environmental insults is regulated at the transcriptional level. The EnvZ sensor protein monitors external signals and modulates the activity of the OmpR response regulator by phosphorylation and dephosphorylation. The OmpR regulator binds to both the *ompC* and *ompF* promoters, but at low concentrations of OmpR-P, *ompF* is activated, while at high concentrations of OmpR-P, *ompF* is repressed and *ompC* is activated. Additional transcriptional control in response to nutrient availability is exerted by the leucine-responsive regulatory protein LRP, a global regulator that negatively regulates *ompC* transcription.

As mentioned above, *ompF* expression is also regulated at the posttranscriptional level via the MicF RNA, and many different environmental stresses impact the OmpC/OmpF ratio via changes in MicF levels (reviewed in reference 9). The expression of *micF* is increased along with that of *ompC* at high OmpR-P concentrations. The expression of *micF* is also in-

* Corresponding author. Mailing address: NIH, Building 18T, Room 101, 18 Library Dr., MSC 5430, Bethesda, MD 20892-5430. Phone: (301) 402-0968. Fax: (301) 402-0078. E-mail: storz@helix.nih.gov.

† S.C. and A.Z. contributed equally to this study.

TABLE 1. Strains and plasmids used for this study

Strain or plasmid	Relevant genotype	Source or reference
Strains		
JM109	Used as wild type	Stratagene
GSO105	JM109 *ompR101 zhf37*::Tn*10*	This study
BW25113	Used as wild type	8
SC200	BW25113 Δ*micC*::*kan* (Kan^r)	This study
SC201	BW25113 *ompC-luc* (Cm^r)	This study
SC204	BW25113 *ompC-luc*Δ*micC*::*kan* (Kan^r Cm^r)	This study
SC209	BW25113 $ompC_{mutant}$-*luc* (Cm^r)	This study
SC210	BW25113 $ompC_{mutant}$-*luc* Δ*micC*::*kan* (Kan^r Cm^r)	This study
SC216	BW25113 $ompC_{mutant}$-*luc* Δ*micC* (Cm^r)	This study
SC218	BW25113 *ompC-luc* Δ*micC* (Cm^r)	This study
GSO107	BW25113 *hfq-1*::Ω (Cm^r)	This study
Plasmids		
pUC119	Cloning vector (Amp^r)	New England Biolabs
pUC-micC	pUC119 carrying ≈410-bp *micC* region (Amp^r)	This study
pAlter-Ex2	p15A origin cloning vector (Tet^r)	Promega
pAE-micC	pAlter-Ex2 carrying ~410-bp *micC* region (Tet^r)	This study
pAE-$micC_{mutant}$	pAlter-Ex2 carrying ~410-bp mutated *micC* region (Tet^r)	This study
pSP-luc+	Cloning vector with luciferase reporter gene (Amp^r)	Promega
pSP-ompC	*ompC* mRNA fused to *luc* in pSP-luc+ (Amp^r)	This study
pSP-$ompC_{mutant}$	Mutated *ompC* mRNA fused to *luc* in pSP-luc+ (Amp^r)	This study
pSP-ompC (cat)	*ompC* mRNA fused to *luc* in pSP-luc+(Cm^r)	This study
pSP-$ompC_{mutant}$ (cat)	Mutated *ompC* mRNA fused to *luc* in pSP-luc+ (Cm^r)	This study
pKD3	Plasmid carrying *cat* gene cassette and oriRγ origin (Cm^r)	8
pKD4	Plasmid carrying *kan* gene cassette and oriRγ origin (Kan^r)	8
pKD46	Red recombinase expression plasmid (Amp^r)	8
pCP20	FLP recombinase expression plasmid (Amp^r)	8
pGEM-2	Cloning vector (Amp^r)	Promega
pGEM-micC	pGEM-2 carrying *micC* gene (Amp^r)	This study
pGEM-$micC_{mutant}$	pGEM-2 carrying *micC* mutant gene (Amp^r)	This study
pGEM-ompC	pGEM-2 carrying *ompC* gene (Amp^r)	This study
pGEM-micF	pGEM-2 carrying *micF* gene (Amp^r)	36
pSP64	Cloning vector (Amp^r)	Promega
pSP64-dsrA	pSP64 carrying *dsrA* gene (Amp^r)	This study

duced by toxic agents, such as paraquat and weak acids, by the SoxS, MarA, and Rob transcription factors, which bind to the same sequence element in the *micF* promoter. MicF RNA levels increase at high temperatures, although the mechanism by which this occurs is not known. As a consequence of MicF induction, high osmolarities, exposures to toxic agents, and high temperatures all indirectly lead to decreased OmpF levels. Since the *micF* gene is repressed by LRP along with *ompC*, LRP repression indirectly leads to increased OmpF levels. Finally, the H-NS-like StpA protein appears to impact OmpF levels through the destabilization of *micF* RNA. Thus, multiple regulatory pathways converge at MicF, leading to changes in the OmpF/OmpC ratio.

In a previous genome-wide search for novel small RNAs, Chen et al. identified a DNA region denoted IS063 that is located between the *ompN* porin gene and a gene of unknown function (*ydbK*) and that is transcribed into a short RNA transcript that lacks the capacity to be translated (7). Using BLAST searches, we found that the small RNA shows complementarity to the leader sequence of the *ompC* mRNA. We postulated that the small RNA may regulate *ompC* expression in the same fashion that MicF regulates *ompF*, and thus we named the small RNA the MicC RNA. Here we present evidence that MicC, which is conserved in *Shigella*, *Salmonella*, and *Klebsiella*, inhibits *ompC* expression at the posttranscriptional level.

MATERIALS AND METHODS

Plasmids and bacterial strains. Standard molecular biology procedures were used for the isolation of genomic DNAs and plasmids, for restriction digests, for molecular cloning, and for transformation by electroporation or heat shock. *Taq* polymerase was used to amplify DNA fragments. The *ompR101* mutant allele linked to *zhf37*::Tn*10* (22) was moved into strain JM109 by P1 transduction (to create GSO105). The *hfq-1*::Ω mutant allele (26) was moved into strain BW25113 by P1 transduction (GSO107). All other strains with gene deletions or mutations on the chromosome were constructed by a one-step method for gene inactivation in *E. coli* by using PCR products and BW25113 transformed with pKD46 and pCP20 (8). After mutants were generated, PCR was routinely used to confirm that the mutated regions had the expected sizes. Some of the PCR products also were sequenced to confirm the presence of mutations and fusions. All of the plasmids and bacterial strains used for this study are listed in Table 1. The sequences of all oligonucleotide primers used for this study are given at the following web site: http://dir2.nichd.nih.gov/nichd/cbmb/segr/segrPublications.html.

For overexpression of the MicC RNA, an ~410-bp DNA fragment (from 180 bp upstream to 110 bp downstream) of the *micC* gene was amplified from JM109 genomic DNA by the use of primers IS063-Bm and IS063-Ec and was then cloned into pUC119 (pUC-micC) and into pAlter-Ex2 (pAE-micC) after digestion with BamHI and EcoRI. For the generation of a *micC* mutant plasmid, a 200-bp fragment was amplified with primers IS063-Bm and MicC-PacRev and a 210-bp fragment was amplified with primers IS063-Ec and MicC-PacI. These two fragments were coligated into pAlter-Ex2 after digestion with PacI, BamHI, and EcoRI (pAE-$micC_{mutant}$).

For construction of a *micC* deletion mutant (SC200), primers IS063-P1 and IS063-P2 were used to amplify the kanamycin resistance gene (Kan^r) from pKD4 together with sequences flanking the *micC* gene. This fragment was then used for

the linear transformation of strain BW25113. For unknown reasons, we found this insertion to be recalcitrant to transduction by P1.

The *ompC-luc* fusion strains were constructed by first creating the fusions in pSP-luc+ and then using amplified portions of the plasmids for linear transformation. For the wild-type *ompC-luc* fusion, a 250-bp fragment containing the transcriptional and translational elements of *ompC* was amplified from the genomic DNA with primers OmpC-Nde2 and OmpC-Nco and was then cloned into pSP-luc+ after digestion with NdeI and NcoI (pSP-ompC). For the mutant *ompC-luc* fusion, a 160-bp fragment was amplified with primers OmpC-Nde2 and OmpC-PacI and a second fragment was made by annealing two oligonucleotides, OmpC-Mut3 and OmpC-Mut4. The two fragments were coligated into pSP-luc+ after digestion with PacI, NdeI, and NcoI (pSP-ompC$_{mutant}$). A 900-bp *cat* cassette obtained by digesting pKD3 with XbaI was cloned into pSP-ompC and pSP-ompC$_{mutant}$ to generate derivatives carrying chloramphenicol resistance (Cm^r). The *cat* genes in both plasmids had the same orientations relative to the reporter genes. Fragments of the Cm^r plasmids were generated by the use of primers Ybak-OmpC and Ybak-luc+ and were used to transform BW25113 to give strains SC201 and SC209. The *micC* deletion derivatives of SC201 (SC204) and SC209 (SC210) were generated with the PCR product used to make SC200. The Kan^r markers in SC204 and SC210 were eliminated with pCP20 to create SC218 and SC216, respectively.

For in vitro synthesis of the *ompC* RNA, the 5′ end of the *ompC* gene (from −79 to +126) was amplified from MC4100 chromosomal DNA by a PCR with primers OmpC-Ec and OmpC-Hd. The PCR fragment was digested with EcoRI and HindIII and then cloned into the corresponding sites of pGEM-2 (pGEM-ompC). For in vitro synthesis of the wild-type MicC RNA, the entire *micC* coding sequence was amplified from MC4100 genomic DNA with primers MicC-Ec and MicC-Hd. The PCR fragment was digested with EcoRI and HindIII and then cloned into the corresponding sites of pGEM-2 (pGEM-micC). For the in vitro synthesis of mutant MicC RNA, site-directed mutagenesis (Stratagene, La Jolla, Calif.) was performed by using pGEM-micC as a DNA template and primers MicCmut2A and MicCmut2B (pGEM-micC$_{mutant}$).

To generate a probe for DsrA, we amplified the *dsrA* gene from JM109 genomic DNA by using primers DsrA-Ec and DsrA-Hd and then cloned it into the pSP64 vector (Promega) after digestion with EcoRI and HindIII (pSP64-dsrA).

Growth conditions. Unless otherwise specified, all strains were grown in Luria-Bertani (LB) broth or on LB agar containing appropriate antibiotics (23). M9-glycerol containing 1× M9 salts (23), 0.2% glycerol (vol/vol), 1 mM $MgSO_4$, 0.1 mM $CaCl_2$, and 2 μg of vitamin B1/ml was used as minimal medium.

Northern analysis. For Fig. 1, total cellular RNAs were isolated by the use of Trizol reagent (Invitrogen). For Fig. 7, total and immunoprecipitated RNAs were isolated by phenol-chloroform extraction and ethanol precipitation. The RNAs were fractionated in an 8% polyacrylamide–8 M urea gel and transferred to Zeta Probe blotting membranes for MicC blots (Bio-Rad Laboratories, Hercules, Calif.) or to Hybond N membranes for MicF and DsrA blots (Amersham Biosciences, Piscataway, N.J.). A MicC Northern oligonucleotide capable of hybridizing to MicC was labeled at the 5′ end with ^{32}P by the use of T4 polynucleotide kinase. The uniformly ^{32}P-labeled MicF RNA probe was generated by using T7 RNA polymerase to transcribe plasmid pGEM-micF (36) linearized with EcoRI. The uniformly ^{32}P-labeled DsrA RNA probe was generated by using SP6 RNA polymerase to transcribe plasmid pSP64-dsrA linearized with EcoRI. Zeta Probe blotting membranes were prehybridized and hybridized in Ultrahyb Oligo buffer (Ambion, Austin, Tex.) at 45°C. Hybond N membranes were prehybridized and hybridized in buffer containing 50% formamide, 1.5× SSPE (1× SSPE is 0.18 M NaCl, 10 mM NaH_2PO_4, and 1 mM EDTA [pH 7.7]), 1% sodium dodecyl sulfate (SDS), and 0.5% dry milk at 55°C. All membranes were washed twice with 4× SSC (1× SSC is 0.15 M NaCl plus 0.015 M sodium citrate)–0.1% SDS at room temperature followed by two 25-min washes with 0.1× SSC–0.1% SDS at 45°C for Zeta Probe blotting membranes and at 55°C for Hybond N membranes.

Primer extension analysis. Primer extension assays were performed with primer OmpC-N1 labeled at the 5′ end with P^{33}, RetroScript reverse transcriptase (Ambion), and total RNA isolated from JM109 cells grown overnight in LB medium (to an optical density at 600 nm [OD_{600}] of 1.2) at room temperature. The total RNA (~10 μg) was isolated from JM109 by use of an RNeasy kit (Qiagen, Valencia, Calif.) and was then incubated with ~10 ng of the primer, 100 U of enzyme, a 0.12 μM concentration of each deoxynucleoside triphosphate, and 0.5 U of RNase inhibitor in 50 mM Tris buffer, pH 8.3, containing 75 mM KCl, 5 mM dithiothreitol, and 3 mM $MgCl_2$ (20-μl reaction volume). The reaction was terminated after 1 h and loaded onto a QuickPoint mini sequencing gel (Invitrogen) together with a sequencing ladder generated from plasmid pIS063 by using the same primer and the DNA sequencing kit of the *fmol* DNA cycle sequencing system (Promega, Madison, Wis.).

3′ RACE analysis. We performed 3′ rapid amplification of cDNA ends (3′ RACE) as described previously (4), using total RNA isolated from JM109 cells grown in LB medium to stationary phase (OD_{600} = 2.0) at 24°C. The total RNA (20 μg) was dephosphorylated with bacterial alkaline phosphatase (Invitrogen) and ligated with a 3′ RNA adapter (E1). cDNA was synthesized by reverse transcription with a primer complementary to the E1 RNA adapter (E4) by use of the Thermoscript RT-PCR system (Invitrogen) according to the manufacturer's instructions. After an RNase H treatment, the reverse transcription products were amplified by PCR with a *micC* gene-specific primer (MicC-RACE) and the adapter-specific primer (E4) and were cloned into the pCR2.1 TOPO TA vector (Invitrogen). The 3′ end of the MicC RNA was identified by DNA sequencing.

Luciferase assays. For assays of the strains carrying *ompC-luc* fusions, overnight cultures were diluted 1:100 in fresh LB medium and incubated at 37°C for 6 h before being harvested. Activities were measured by use of a luciferase assay system (Promega) for bacteria, with slight modifications. The cell culture was diluted four times immediately before being mixed with carrier cells (BW25113), flash frozen, and lysed. The luminescence obtained after mixing 20 μl of the cell lysate and 100 μl of the assay reagent was measured in a microplate TopCount NXT scintillation counter (Perkin-Elmer LAS, Shelton, Conn.). The protein concentration of each cell lysate was measured by use of the noninterfering BCA protein assay reagent (Pierce, Rockford, Ill.). The luciferase activity is given in counting units normalized to the protein concentration for each protein extract. For strains expressing MicC and its mutant from plasmids, the host strains were freshly transformed. Cultures that were started from single colonies picked within 18 h after transformation and grown in LB broth with antibiotics for 12 h were used for the dilutions into fresh LB broth.

SDS-polyacrylamide gel electrophoresis. To determine the levels of the OmpC protein, we incubated cells in LB medium to exponential phase (OD_{600} = 0.6) at 24°C and then prepared the cell envelopes as described previously (6, 17). The proteins were separated by SDS-polyacrylamide gel electrophoresis in 12% polyacrylamide gels containing 4 M urea and were stained with GelCode Blue stain (Pierce).

Toeprinting assays. Toeprinting assays were performed by a modification of a previously described method (2). For the generation of OmpC, MicC, and MicC$_{mutant}$ RNAs, pGEM plasmids were linearized with HindIII, and the RNAs were synthesized by in vitro transcription with SP6 RNA polymerase. Annealing mixtures contained 0.2 pmol of *ompC* RNA, 0.6 pmol of 5′-end-labeled oligonucleotide OmpC-RT complementary to *ompC* RNA, and 1.2 pmol of wild-type MicC oligo, mutant MicC oligo #1, mutant MicC oligo #2, or in vitro-synthesized wild-type MicC or mutant MicC RNA. The mixtures were heated for 3 min at 65°C and then chilled in ice water for 15 min. The extension reactions contained the annealing mixtures, a 0.5 mM concentration of each deoxynucleoside triphosphate, 3 pmol of preactivated (30 min at 37°C) 30S ribosomal subunits (kindly provided by Steven Ringquist), 20 mM Tris-HCl, 10 mM magnesium acetate, 0.1 M NH_4Cl, 0.5 mM EDTA, and 2.5 mM β-mercaptoethanol. After preincubation for 5 min at 37°C, 12 pmol of uncharged fMet-tRNA was added, and the reactions were incubated for an additional 10 min. Reverse transcriptase (1 U; Invitrogen) was added, and cDNA synthesis was allowed to proceed for 15 min. The cDNA products were analyzed in 8% polyacrylamide gels containing 8 M urea.

Immunoprecipitation. Cell extracts were prepared from cultures of BW25113 or GS107 grown in LB medium at 24°C to exponential phase. Immunoprecipitations were performed as described previously (35), using 20 μl of an Hfq antiserum or preimmune serum, 24 mg of protein A-Sepharose (Amersham Biosciences), and 200 μl of cell extract.

RESULTS

A 109-nucleotide RNA encoded between *ompN* and *ydbK*. In a previous computational search for novel small RNA genes in the *E. coli* genome, Chen et al. predicted that a small RNA might be expressed from a σ^{70} promoter with a −10 sequence at position 1435142 and with a putative terminator at position 1435259, and indeed they detected a small RNA of ~100 nucleotides on Northern blots probed with a PCR-generated fragment (7). For this study, we set out to characterize this small RNA by examining its expression, determining its 5′ and 3′ ends, searching for homologs and complementary sequences

by comparative genomic analysis, and assaying the phenotypes associated with decreased and increased expression of the RNA. Although the RNA was initially designated IS063, we have renamed it MicC for the reasons described below.

To examine the expression profile of the MicC RNA, we prepared total cellular RNAs from JM109 cells grown under a series of growth conditions and analyzed them on Northern blots probed with a labeled antisense oligonucleotide specific for the predicted transcript. As shown in Fig. 1A, expression of the MicC RNA was induced by growth at 24°C in both stationary- and exponential-phase cells (lanes 1 and 2). The level of the RNA was also elevated in cells grown to exponential phase in minimal medium with glycerol as the carbon source (lane 10) and was elevated further when these cells were exposed to osmotic shock (lanes 11). To a lesser degree, the expression of the RNA was induced in cells grown in LB broth and exposed to paraquat (lane 6). The MicC RNA was undetectable in stationary-phase cells grown in either LB or minimal medium at 37°C (lanes 3 and 9) and was only present at very low levels during exponential growth in LB medium at 37°C (lane 4), with no further induction by heat shock (lane 5) or exposure to H_2O_2 (lane 7) or a low pH (lane 8). Interestingly, under most of the conditions tested, the expression of the MicC RNA was opposite to the expression of the MicF RNA. Since OmpR has been reported to modulate MicF expression (reviewed in reference 9), we also examined MicC expression in an *ompR* mutant strain (Fig. 1B). As expected, MicF RNA levels were lower in the *ompR* mutant strain. On the other hand, MicC RNA levels were increased, indicating that OmpR, directly or indirectly, represses MicC expression.

We also determined the 5′ and 3′ ends of the small RNA. To identify the 5′ end, we performed a primer extension analysis with total RNAs isolated from JM109 cells (Fig. 2A). A strong signal was detected corresponding to transcription starting at a G at position 1435145 (shown in bold and in a larger font in Fig. 2B), in agreement with our promoter prediction. The 3′ end was mapped to position 1435253 by 3′ RACE. Thus, the 3′ stem-loop terminator structure was retained even though some of the 3′ U residues were removed, which is a common feature among the mature small RNAs of *E. coli* (12). The 5′ and 3′ ends corresponded to a 109-nucleotide RNA, in agreement with our Northern analysis.

The small RNA is encoded by the intergenic region between two open reading frames whose gene products are poorly characterized (Fig. 2C). The *ompN* gene is transcribed divergently upstream of *micC*. This gene encodes an outer membrane protein that has the highest similarity to OmpC (65% identity) (20). The *ydbK* gene, which is located downstream of *micC* and transcribed in the same direction as *ompN*, encodes a probable pyruvate-flavodoxin oxidoreductase. The *ompN-micC-ydbK* region on the K-12 chromosome is well conserved in *E. coli* O157:H7, with over 98% identity. MicC homologs were also found in all of the sequenced *Shigella*, *Salmonella*, and *Klebsiella* genomes, with the highest level of conservation encompassing the first 20 nucleotides and the terminator structure (Fig. 2D). The −10 and −35 sequences of the *micC* promoter are also conserved in the alignment of the entire intergenic sequence (http://dir2.nichd.nih.gov/nichd/cbmb/segr/segrPublications.html).

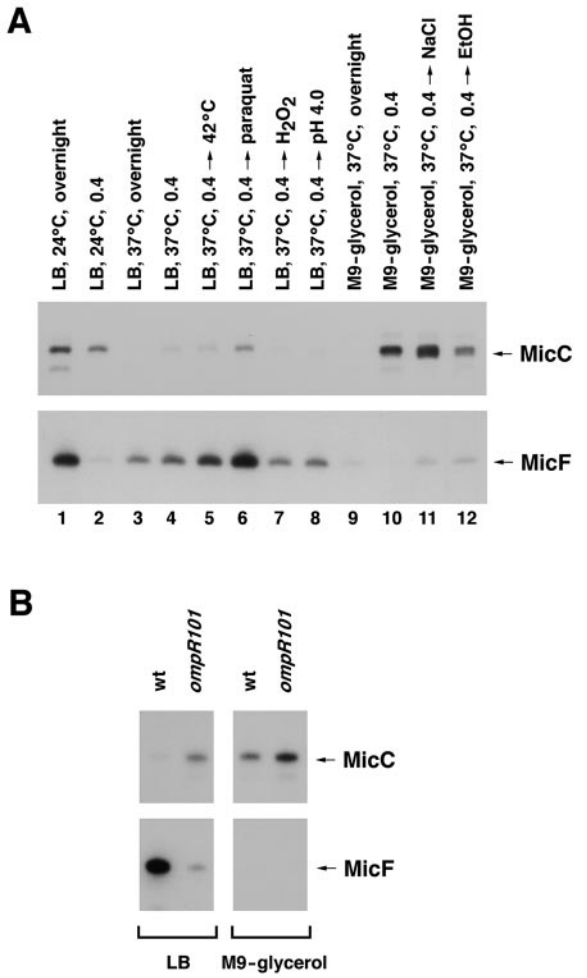

FIG. 1. MicC and MicF RNA levels under various growth conditions. (A) Levels of MicC and MicF RNAs in JM109 cells grown under different growth conditions as follows: stationary phase (overnight; lane 1) or exponential phase (OD_{600} = 0.4; lane 2) in LB medium at 24°C; stationary phase (lane 3) or exponential phase (lane 4) in LB medium at 37°C; growth in LB medium at 37°C to exponential phase and then a switch to 42°C for 20 min (lane 5), a treatment with 0.5 mM paraquat for 20 min (lane 6), a treatment with 0.2 mM H_2O_2 for 5 min (lane 7), or a switch to pH 4.5 for 20 min (lane 8); stationary phase (lane 9) or exponential phase (lane 10) in M9-glycerol medium at 37°C; growth in M9-glycerol medium at 37°C to exponential phase and then a treatment with 0.3 mM NaCl (lane 11) or 10% ethanol (lane 12) for 20 min. The bands corresponding to the MicC and MicF RNAs are denoted by arrows. (B) Levels of MicC and MicF RNAs in wild-type and *ompR* mutant strains grown to exponential phase (OD_{600} = 0.4) in LB medium or M9-glycerol medium at 37°C. For both panels, 10-μg samples of total RNA were fractionated in 8% polyacrylamide–urea gels and analyzed by Northern hybridization with a labeled oligonucleotide complementary to MicC or a labeled RNA complementary to MicF.

Complementarity between MicC and 5′ leader of *ompC* mRNA. We next looked for sequences that are complementary to MicC in the *E. coli* genome. A BLASTN search revealed that 16 continuous nucleotides starting from the 5′ end of the small RNA are complementary to the sequence adjacent to the presumed ribosomal binding site of the *ompC* gene, which encodes major outer membrane protein C (Fig. 3A). Thus,

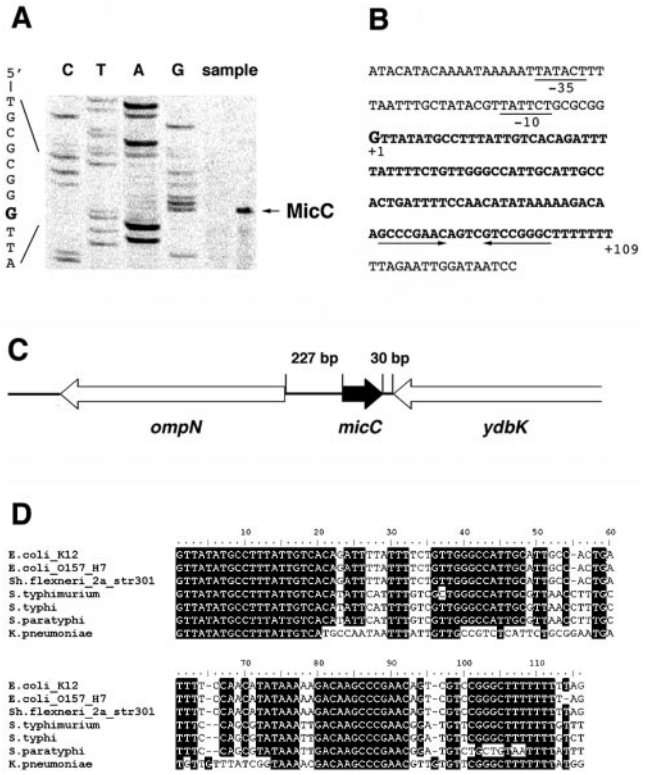

FIG. 2. Sequence of MicC RNA. (A) Primer extension analysis of MicC RNA. Reverse transcriptase reactions were carried out as described in Materials and Methods, using total RNA isolated from JM109 cells grown overnight in LB medium at room temperature. The transcription initiation site corresponding to a G is indicated with an arrow. (B) Sequence of *micC* gene in *E. coli* K-12. The −10 and −35 promoter sequences are underlined, and bold letters denote the *micC* coding sequence. The stem-loop of the predicted terminator is indicated by arrows. (C) Chromosomal position of *micC*. *micC* is transcribed clockwise on the chromosome on the strand opposite the adjacent *ompN* and *ydbK* genes. (D) Alignment of *micC* homologs by the CLUSTALW program (http://molbio.info.nih.gov/molbio/gcglite/clustalw18.html).

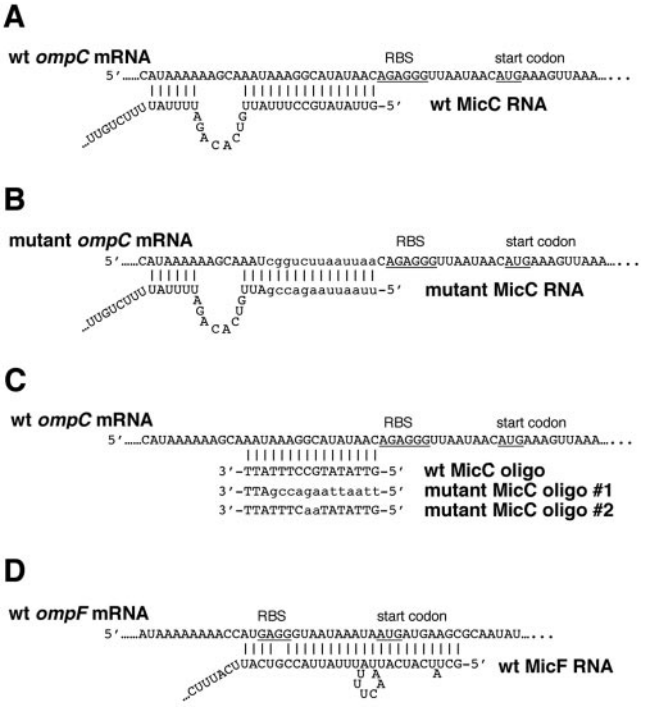

FIG. 3. Proposed formation of MicC-*ompC* and MicF-*ompF* duplexes. (A) Base pairing between wild-type *ompC* mRNA leader and wild-type MicC RNA (pAE-micC) identified by a BLASTN search (http://www.ncbi.nlm.nih.gov/BLAST/) of the *E. coli* genome. (B) Base pairing between a mutant *ompC* mRNA leader and a mutant MicC RNA (pAE-micC$_{mutant}$). The sequence of the PacI restriction site is UUAAUUAA. (C) Base pairing between wild-type *ompC* mRNA leader and wild-type and mutant oligonucleotides. (D) Base pairing between wild-type *ompF* mRNA leader and wild-type MicF RNA (24). Ribosome-binding sites (RBS) and start codons for *ompC* and *ompF* are underlined, and the mutant sequences are indicated with lowercase letters.

MicC could potentially form base pairs with the *ompC* mRNA, suggesting that it may act as an antisense regulator. Upon allowing a gap, the potential antisense region can be extended another six nucleotides upstream. Since the *micC* and *ompC* genes are located at different genetic loci and are produced from two separate transcriptional units, the situation strongly mimics the MicF regulation of *ompF* (Fig. 3D). We also noted that the *micC-ompN* gene organization resembles the *micF-ompC* gene organization. These similarities encouraged us to test the hypothesis that MicC regulates *ompC* expression.

Effects of *micC* overexpression and deletion. To assay the effects of eliminating MicC RNA expression, we created a mutant with the entire *micC* sequence deleted (positions 1435155 to 1435241) in the background of *E. coli* K-12 strain BW25113 (SC200). Since the stem-loop sequence comprising the *micC* terminator is likely to also serve as a terminator for the adjacent *ydbK* gene, the complete *micC* deletion may have affected expression of the unknown YdbK protein. Thus, we constructed a second deletion strain in which only the 5′ end of *micC* was deleted (positions 1435155 to 1435201), but we found that the two strains had similar phenotypes in all of the assays that we performed (data not shown). The *micC* region (~410 bp) was also cloned into a plasmid, pAlter-Ex2 (pAE-micC), in strain BW25113 to create an overexpression strain. Northern analysis confirmed that MicC was absent from SC200 and that the *micC* RNA was overexpressed about 10-fold by pAE-micC (data not shown). Neither the deletion nor the overexpression strain showed significant variations in growth compared to the parent strain under various growth conditions.

To test whether MicC had effects on the expression of the proposed target *ompC* mRNA, we constructed an *ompC-luc* translational fusion in which *luc* was fused in frame to the start codon of *ompC* (Fig. 4A). In this construct, the expression of luciferase was under the control of the transcriptional and translational elements of *ompC*, including three OmpR binding sites (27). The fusion was integrated into the intergenic region between genes *ybaK* and *ybaP* (positions 506382 to 506473) to avoid compensatory changes in the expression of other porin genes associated with the disruption of *ompC*. A previous deletion of the *ybaK-ybaP* region on the chromosome did not result in any observable phenotypes (data not shown). The *ompC-luc* fusion strain was transformed with the MicC

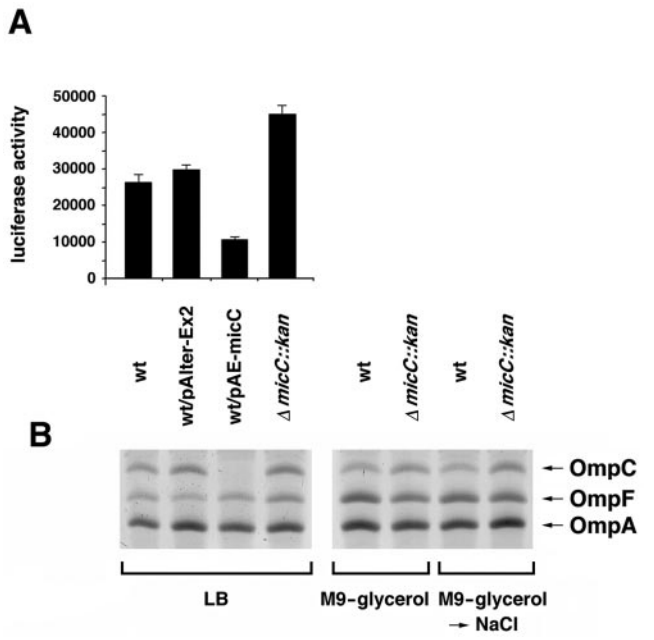

FIG. 4. Effects of increased and decreased expression of MicC on *ompC* expression. (A) Luciferase activities (luminescence counts per microgram of protein) for the wild-type strain (SC201), the wild-type strain carrying the control pAlter-Ex2 vector, the wild-type strain carrying pAE-micC, and the corresponding *micC* deletion strain (SC204), with each grown for 6 h in LB medium at 37°C. The experiment was repeated three times, and averages and standard deviations are presented. (B) Levels of OmpC, OmpF, and OmpA proteins in the wild-type strain (BW25113), the wild-type strain carrying the control pAlter-Ex2 vector, the wild-type strain carrying pAE-micC, and the corresponding *micC* deletion strain (SC200), with each grown to an OD_{600} of 0.6 in LB medium at 24°C or an OD_{600} of 0.4 in M9-glycerol medium at 37°C and then treated with 0.3 mM NaCl for 20 min. The strains assayed in panel B were the same as the strains assayed in panel A, except they did not carry the *ompC-luc* fusion.

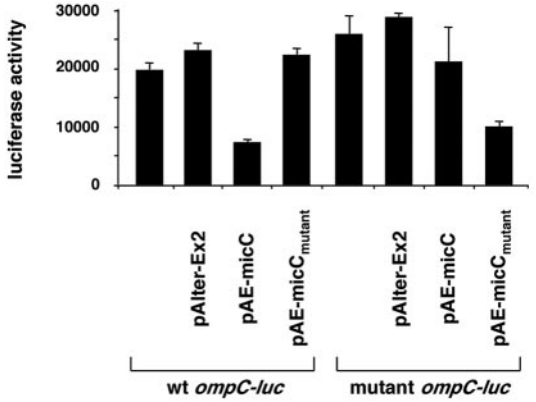

FIG. 5. Effects of compensatory mutations. Luciferase activities (luminescence counts per microgram of protein) for the *micC* deletion strain carrying the wild-type *ompC-luc* fusion (SC218) or the mutant *ompC-luc* fusion (SC216) and transformed with pAlter-Ex2, pAE-micC, or pAE-micC$_{mutant}$ are given. The experiment was repeated three times, and averages and standard deviations are presented.

overexpression plasmid (pAE-micC) and the corresponding control plasmid. The *micC* deletion was also moved into the fusion strain. The different *ompC-luc* strains were grown for 6 h in LB medium, and luciferase activities were assayed and normalized to the total protein concentrations. These assays showed that there was a 60% reduction in the expression of the *ompC-luc* fusion when MicC was overexpressed, while there was a 1.5- to 2.0-fold increase in *ompC* expression when *micC* was deleted (Fig. 4A). Similar increases and decreases in activity were observed for cells grown in minimal medium, although the overall levels of activity were lower, possibly due to some unknown expression problem associated with the *luc* gene in minimal medium (data not shown).

The effects of MicC overexpression and the *micC* deletion on *ompC* expression were also examined by monitoring OmpC protein levels directly in urea gels by using outer membrane protein preparations from cells grown to exponential phase. As shown in Fig. 4B, the overexpression of MicC clearly resulted in reduced OmpC protein levels, while the deletion of *micC* led to a twofold increase in OmpC levels, again suggesting that the MicC RNA represses *ompC* expression. Overexpression of the small RNA and deletion of the *micC* gene did not impact the expression of the OmpA and OmpF porins, which were also detected under these conditions.

Duplex formation between MicC and *ompC-luc*. To further test for base pairing between MicC and the *ompC* mRNA, we separately mutated the regions of base pairing and investigated the effects of the mutations on *ompC-luc* gene expression. We scrambled 10 nucleotides in the base pairing region of the *ompC* mRNA leader while retaining the GC composition (25%) to create a mutated *ompC-luc* fusion in the plasmid. The mutated region had a PacI restriction site as its signature (Fig. 3B). The wild-type and mutant *ompC-luc* constructs were integrated into the *ybaK-ybaP* intergenic region on the chromosome by a double crossover. The *micC* deletion mutation subsequently was also recombined into these strains. In addition, we mutated the complementary nucleotides of the *micC* gene encoded on pAE-micC (generating pAE-micC$_{mutant}$) to allow the mutant MicC RNA to form base pairs with the mutant, but not the wild-type, *ompC-luc* fusion (Fig. 3B). The mutant *micC* gene also carried a signature PacI site. The pAlter-Ex2 vector, pAE-micC, and pAE-micC$_{mutant}$ were separately transformed into the wild-type and mutant *ompC-luc* fusion strains carrying the *micC* deletion. The transformants and the nontransformed parental strains were then grown for 6 h, and luciferase activities were measured as described above.

As shown in Fig. 5, we again observed that wild-type MicC repressed wild-type *ompC-luc* expression about twofold (wt *ompC-luc*/pAE-micC). The overexpression of mutant MicC repressed the mutated *ompC-luc* fusion to a similar degree (mutant *ompC-luc*/pAE-micC$_{mutant}$). This repression was not seen when wild-type MicC was expressed in the mutant *ompC-luc* strain (mutant *ompC-luc*/pAE-micC) or when mutant MicC was expressed in the wild-type *ompC-luc* strain (wt *ompC-luc*/pAE-micC$_{mutant}$). The luciferase activities in the last two strains were almost identical to the activity levels seen for the untransformed strains as well as for the strains carrying the control vector. We thus concluded that the wild-type *ompC-luc* mRNA forms base pairs with and is repressed by wild-type MicC and that the antisense regulation of this reporter gene

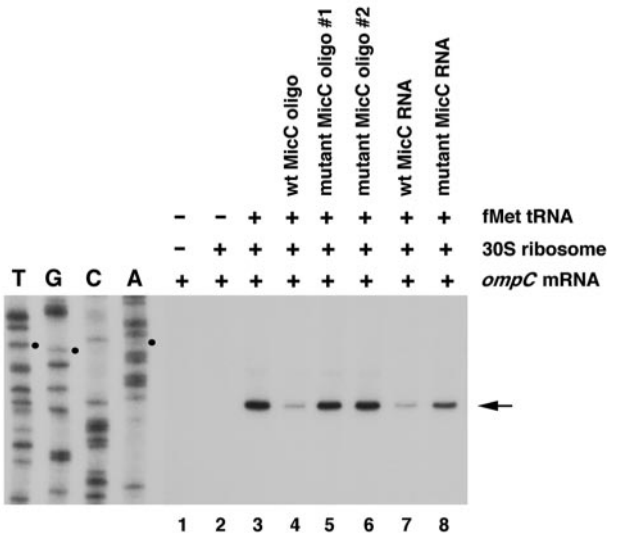

FIG. 6. Toeprinting analysis of 30S ribosomal subunit binding to *ompC* mRNA. The arrow indicates the toeprint signal at the C residue, and the three small dots indicate the AUG start codon. The DNA sequencing reactions were carried out with the same end-labeled oligonucleotide used in the toeprinting assay.

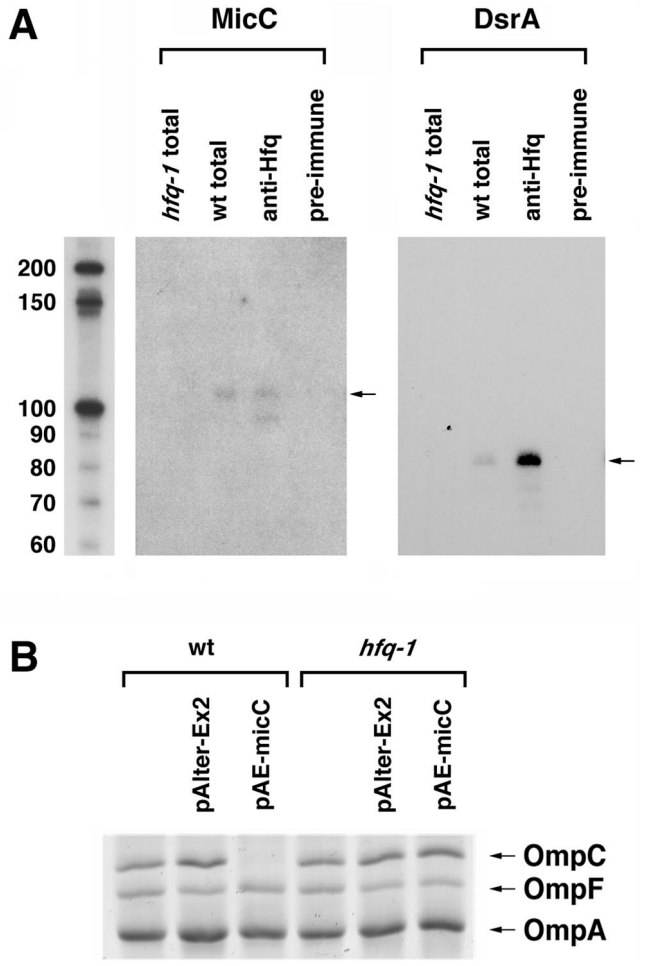

FIG. 7. Requirement of Hfq for MicC repression of *ompC*. (A) Hfq binding to MicC RNA. Cell extracts were prepared from wild-type (BW25113) or *hfq-1* mutant (GSO107) cells grown to an OD_{600} of 0.6 in LB medium at 24°C. Immunoprecipitations were carried out with the wild-type extracts and an Hfq antiserum or a preimmune serum and were compared to total RNAs from 1/10 extract equivalents of the wild-type and *hfq-1* mutant RNAs. The levels of MicC and the DsrA positive control were determined by Northern hybridization. (B) Levels of OmpC, OmpF, and OmpA proteins in wild-type and *hfq-1* mutant strains without and with pAlter-Ex2 or pAE-micC grown to an OD_{600} of 0.6 in LB medium at 24°C.

expression was only restored in a strain carrying the corresponding compensatory mutations.

MicC inhibits 30S ribosome binding to *ompC* mRNA. Unlike the region of MicF-*ompF* base pairing (Fig. 3D), the region of MicC-*ompC* base pairing does not overlap the ribosome binding site and the *ompC* start codon (Fig. 3A). Interactions involving nucleotides in the mRNA leader other than those of the ribosome binding site and the start codon have been shown to inhibit translation in other cases, such as that of the Trap-regulated genes in *Bacillus* and CsrA-regulated genes in *E. coli* (5, 13). However, we wanted to directly test whether MicC could block ribosome binding. Thus, we performed a primer extension inhibition assay, also called a toeprinting assay, to examine whether MicC-*ompC* RNA base pairing would inhibit the formation of the translational initiation complex. In vitro-synthesized *ompC* mRNA was annealed to an end-labeled primer complementary to a region 97 to 121 nucleotides downstream of the *ompC* translation start site. This complex was then incubated with 30S ribosome subunits in the presence or absence of uncharged fMet-tRNA. An analysis of the extension products revealed one ribosome-induced, fMet-tRNA-dependent termination site at the C residue 15 nucleotides downstream of the AUG start codon (Fig. 6, lane 3). This toeprint signal was decreased when a wild-type MicC oligonucleotide or RNA was added prior to incubation with the 30S subunits and the uncharged fMet-tRNA (lanes 4 and 7). In contrast, the addition of MicC mutant oligonucleotides (lanes 5 and 6) or a mutant RNA (lane 8) did not lead to a decrease in the toeprint, indicating that the mutant oligonucleotides and RNA were unable to repress 30S binding. The mutant RNA and mutant oligonucleotide 1 carried the same mutations as pAE-micC$_{mutant}$, while mutant oligonucleotide 2 contained a GC→AA change (Fig. 3B and C). Interestingly, we did not detect an obvious difference between the two mutant oligonucleotides (Fig. 6, lanes 5 and 6), despite that fact that oligonucleotide 1 had a 10-nucleotide mismatch while oligonucleotide 2 only had a 2-nucleotide mismatch. This suggests that the GC dinucleotide contributes substantial energy to maintaining the small RNA-mRNA duplex. Together, the results demonstrate that MicC inhibits the formation of an *ompC* mRNA-30S ribosome initiation complex.

Hfq requirement for MicC function. All of the *E. coli* small RNAs that act by base pairing have been found to bind the Sm-like Hfq protein, and many have been shown to require Hfq for their function (reviewed in references 25 and 28). Given that MicC represses *ompC* by base pairing, the paradigms suggest that MicC also should bind to Hfq. To directly test whether the MicC RNA is bound by Hfq, we performed a Northern analysis with RNAs isolated from wild-type and *hfq* mutant cells as well as with RNAs immunoprecipitated with

control and Hfq-specific antisera. MicC was indeed detected in the samples from Hfq immunoprecipitation, and the levels of the RNA were decreased in the *hfq* mutant strain, similar to what has been found for other Hfq binding RNAs such as the control DsrA RNA (Fig. 7A). We did note that the MicC RNA was extremely unstable in the cell extracts used for the immunoprecipitation assays. This may explain why MicC was not identified in a global screen for Hfq binding RNAs (36).

To test whether Hfq was required for MicC function, we also examined the effect of MicC overexpression on OmpC protein levels in wild-type and *hfq* mutant cells. The repression of OmpC levels observed for the wild-type strain was diminished in the *hfq* mutant, indicating that Hfq is needed for MicC base pairing with the *ompC* mRNA (Fig. 7B).

DISCUSSION

After the discovery of tens of potential small RNA genes in *E. coli* by our bioinformatics-based strategies and various approaches employed by many other groups (4, 7, 21, 29, 33, 36), work is starting to focus on the characterization of these novel small RNAs. In this paper, we show that a 109-nucleotide RNA identified in a computational screen contributes to the regulation of synthesis of the major outer membrane protein OmpC. MicC inhibits *ompC* expression at the posttranscriptional level by an antisense mechanism that involves the formation of base pairs between 22 nucleotides at the 5′ end of MicC and nucleotides just before the ribosome binding site of the *ompC* mRNA (Fig. 3).

Many parallels can be drawn between the 109-nucleotide MicC RNA and the 93-nucleotide MicF RNA. Both repress the expression of abundant porins by base pairing near the ribosome binding site, thereby blocking translation. Both are also encoded opposite other porin genes in *E. coli*. In addition, the MicF RNA and the corresponding *ompF* target sequence have been detected in *Salmonella enterica* serovar Typhi, *S. enterica* serovar Typhimurium, and *Klebsiella pneumoniae* (10), the same organisms in which MicC homologs are evident. It should be noted, however, that while an outer membrane protein-like open reading frame is present immediately upstream of *micC* in *Klebsiella*, a similar gene is absent from *Salmonella* sp.

Interestingly, the MicC and MicF RNAs were generally expressed under different environmental conditions. As shown in Fig. 1, MicF levels were elevated under most conditions in which MicC levels were low, while MicC levels were highest under those conditions in which MicF levels were low. These observations are in agreement with the previous observation that OmpC and OmpF show reciprocal expression under many environmental conditions (reviewed in reference 19). It should be noted, however, that the regulation of porin expression is complex and that there may be conditions in which similar levels of OmpC and OmpF are needed for growth and survival.

Given the analogies between the MicF regulation of *ompF* and the MicC regulation of *ompC*, it is tempting to speculate that there is a dual transcriptional regulation of *micC* and the adjacent *ompN* gene similar to what is observed for *micF* and the adjacent *ompC* gene. OmpN was characterized as a quiescent porin, with the amounts present in cells grown in rich media under normal laboratory conditions being too small to be detected (20). It was noted that OmpN resembles OmpC in its primary amino acid sequence and channel conductance, while OmpN is more similar to OmpF with respect to the differential uptake of mono- and disaccharides (20). There is no further information concerning the regulation of *ompN* and the functional relevance of OmpN to OmpC. The intergenic space between the *ompN* and *micC* genes is 229 bp, which is slightly shorter than the ~256-bp spacer region between *ompC* and *micF*, and we could not find any sequence elements in the *micC* and *ompN* promoter region that were similar to the OmpR binding sites in the *micF* and *ompC* promoter region (27). However, given the coinduction of *micF* and *ompC* under conditions of high osmolarity, it might be interesting to test whether OmpN expression is increased under conditions in which MicC is maximally induced.

The base pairing between the MicC and MicF RNAs and their targets was more extensive than that observed for most of the *E. coli* small RNAs that act by base pairing. The *ompF* mRNA-MicF RNA duplex has been enzymatically and chemically characterized, and the region of base pairing was found to encompass 24 nucleotides (24). The *ompC* mRNA-MicC RNA interaction involves 16 contiguous nucleotides just before the *ompC* ribosome binding site in the upstream direction and an additional 6 nucleotides further upstream. The consequences of this extensive pairing are not known. As shown in Fig. 7, MicC binds to Hfq and requires the RNA chaperone to repress *ompC*. MicF has also been shown to bind to the RNA chaperone and is likely to require the protein for its function (36).

It is intriguing that small RNAs regulate the expression of two abundant outer membrane proteins, OmpC and OmpF, at a posttranscriptional level. The expression of yet another abundant outer membrane protein, OmpA, has also been shown to be posttranscriptionally regulated. In this case, Hfq binding has been found to stimulate *ompA* mRNA decay (30). Given the association of small RNAs with OmpC and OmpF expression, it is tempting to speculate that the regulation of OmpA expression also involves a *trans*-encoded RNA. A broader issue for future research is determining the advantage of antisense regulation for controlling the synthesis of outer membrane proteins.

ACKNOWLEDGMENTS

We are grateful to M. Goulian for advice on separating the Omp proteins in urea gels, to S. Ringquist for 30S subunits, to B. Wanner and the *E. coli* Genetic Stock Center (EGSC) for providing the *E. coli* one-step gene inactivation system, and to T. A. Hall for providing software to analyze DNA sequences. We thank S. Gottesman and members of the laboratory for helpful discussions and comments on the manuscript.

REFERENCES

1. **Aiba, H., S.-I. Matsuyama, T. Mizuno, and S. Mizushima.** 1987. Function of *micF* as an antisense RNA in osmoregulatory expression of the *ompF* gene in *Escherichia coli*. J. Bacteriol. **169:**3007–3012.
2. **Altuvia, S., D. Weinsterin-Fischer, A. Zhang, L. Postow, and G. Storz.** 1997. A small, stable RNA induced by oxidative stress: role as a pleiotropic regulator and antimutator. Cell **90:**43–53.
3. **Andersen, J., S. A. Forst, K. Zhao, M. Inouye, and N. Delihas.** 1989. The function of *micF* RNA. *micF* RNA is a major factor in the thermal regulation of OmpF protein in *Escherichia coli*. J. Biol. Chem. **264:**17961–17970.
4. **Argaman, L., R. Hershberg, J. Vogel, G. Bejerano, E. G. H. Wagner, H. Margalit, and S. Altuvia.** 2001. Novel small RNA-encoding genes in the intergenic regions of *Escherichia coli*. Curr. Biol. **11:**941–950.

5. **Babitzke, P., and P. Gollnick.** 2001. Posttranscription initiation control of tryptophan metabolism in *Bacillus subtilis* by the Trp RNA-binding attenuation protein (TRAP), anti-TRAP, and RNA structure. J. Bacteriol. **183:** 5795–5802.
6. **Batchelor, E., and M. Goulian.** 2003. Robustness and the cycle of phosphorylation and dephosphorylation in a two-component regulatory system. Proc. Natl. Acad. Sci. USA **21:**691–696.
7. **Chen, S., E. A. Lesnik, A. T. Hall, R. Sampath, R. H. Griffey, D. J. Ecker, and L. B. Blyn.** 2002. A bioinformatics based approach to discover small RNA genes in the *Escherichia coli* genome. BioSystems **65:**157–177.
8. **Datsenko, K. A., and B. L. Wanner.** 2000. One-step inactivation of chromosomal genes in *Escherichia coli* K-12 using PCR products. Proc. Natl. Acad. Sci. USA **97:**6640–6645.
9. **Delihas, N., and S. Forst.** 2001. MicF: an antisense RNA gene involved in response of *Escherichia coli* to global stress factors. J. Mol. Biol. **313:**1–12.
10. **Esterling, L., and N. Delihas.** 1994. The regulatory RNA gene *micF* is present in several species of gram-negative bacteria and is phylogenetically conserved. Mol. Microbiol. **12:**639–646.
11. **Koebnik, R., K. P. Locher, and P. Van Gelder.** 2000. Structure and function of bacterial outer membrane proteins: barrels in a nutshell. Mol. Microbiol. **37:**239–253.
12. **Li, Z., S. Pandit, and M. P. Deutscher.** 1998. 3′-Exoribonucleolytic trimming is a common feature of the maturation of small, stable RNAs in *Escherichia coli*. Proc. Natl. Acad. Sci. USA **95:**2856–2861.
13. **Liu, M. Y., G. Gui, B. Wei, J. F. I. Preston, L. Oakford, U. Yuksel, D. P. Giedroc, and T. Romeo.** 1997. The RNA molecule CsrB binds to the global regulatory protein CsrA and antagonizes its activity in *Escherichia coli*. J. Biol. Chem. **272:**17502–17510.
14. **Massé, E., N. Majdalani, and S. Gottesman.** 2003. Regulatory roles for small RNAs in bacteria. Curr. Opin. Microbiol. **6:**120–124.
15. **Matsuyama, S.-I., and S. Mizushima.** 1985. Construction and characterization of a deletion mutant lacking *micF*, a proposed regulatory gene for OmpF synthesis in *Escherichia coli*. J. Bacteriol. **162:**1196–1202.
16. **Mizuno, T., M.-Y. Chou, and M. Inouye.** 1984. A unique mechanism regulating gene expression: translational inhibition of a complementary RNA transcript (micRNA). Proc. Natl. Acad. Sci. USA **81:**1966–1970.
17. **Morona, R., and P. Reeves.** 1982. The *tolC* locus of *Escherichia coli* affects the expression of three major outer membrane proteins. J. Bacteriol. **150:** 1016–1023.
18. **Nikaido, H.** 2003. Molecular basis of bacterial outer membrane permeability revisited. Microbiol. Mol. Biol. Rev. **67:**593–656.
19. **Pratt, L. A., W. Hsing, K. E. Gibson, and T. J. Silhavy.** 1996. From acids to *osmZ*: multiple factors influence synthesis of the OmpF and OmpC porins in *Escherichia coli*. Mol. Microbiol. **20:**911–917.
20. **Prilipov, A., P. S. Phale, R. Koebnik, C. Widmer, and J. P. Rosenbusch.** 1998. Identification and characterization of two quiescent porin genes, *nmpC* and *ompN*, in *Escherichia coli* B^E. J. Bacteriol. **180:**3388–3392.
21. **Rivas, E., R. J. Klein, T. A. Jones, and S. R. Eddy.** 2001. Computational identification of noncoding RNAs in *E. coli* by comparative genomics. Curr. Biol. **11:**1369–1373.
22. **Russo, F. D., and T. J. Silhavy** 1991. EnvZ controls the concentration of phosphorylated OmpR to mediate osmoregulation of the porin genes. J. Mol. Biol. **5:**567–580.
23. **Sambrook, J., E. F. Fritsch, and T. Maniatis.** 1989. Molecular cloning: a laboratory manual, 2nd ed. Cold Spring Harbor Laboratory Press, Cold Spring Harbor, N.Y.
24. **Schmidt, M., P. Zheng, and N. Delihas.** 1995. Secondary structures of *Escherichia coli* antisense *micF* RNA, the 5′-end of the target *ompF* mRNA, and the RNA/RNA duplex. Biochemistry **34:**3621–3631.
25. **Storz, G., J. A. Opdyke, and A. Zhang.** 2004. Controlling mRNA stability and translation with small, noncoding RNAs. Curr. Opin. Microbiol. **7:**140–144.
26. **Tsui, H. C., G. Feng, and M. E. Winkler.** 1997. Negative regulation of *mutS* and *mutH* repair gene expression by the Hfq and RpoS global regulators of *Escherichia coli* K-12. J. Bacteriol. **179:**7476–7487.
27. **Tsung, K., R. E. Brissette, and M. Inouye.** 1989. Identification of the DNA-binding domain of the OmpR protein required for transcriptional activation of the *ompF* and *ompC* genes of *Escherichia coli* by *in vivo* DNA foot printing. J. Biol. Chem. **264:**10104–10109.
28. **Valentin-Hansen, P., M. Eriksen, and C. Udesen.** 2004. The bacterial Sm-like protein Hfq: a key player in RNA transactions. Mol. Microbiol. **51:**1525–1533.
29. **Vogel, J., V. Bartels, T. H. Tang, G. Churakov, J. G. Slagter-Jäger, A. Hüttenhofer, and E. G. H. Wagner.** 2003. RNomics in *Escherichia coli* detects new sRNA species and indicates parallel transcriptional output in bacteria. Nucleic Acids Res. **31:**6435–6443.
30. **Vytvytska, O., I. Moll, V. R. Kaberdin, A. von Gabain, and U. Blasi.** 2000. Hfq (HF1) stimulates *ompA* mRNA decay by interfering with ribosome binding. Genes Dev. **14:**1109–1118.
31. **Wagner, E. G. H., S. Altuvia, and P. Romby.** 2002. Antisense RNAs in bacteria and their genetic elements. Adv. Genet. **46:**361–398.
32. **Wassarman, K. M.** 2002. Small RNAs in bacteria: diverse regulators of gene expression in response to environmental changes. Cell **109:**141–144.
33. **Wassarman, K. M., F. Repoila, C. Rosenow, G. Storz, and S. Gottesman.** 2001. Identification of novel small RNAs using comparative genomics and microarrays. Genes Dev. **15:**1637–1651.
34. **Wassarman, K. M., A. Zhang, and G. Storz.** 1999. Small RNAs in *Escherichia coli*. Trends Microbiol. **7:**37–45.
35. **Zhang, A., K. M. Wassarman, J. Ortega, A. C. Steven, and G. Storz.** 2002. The Sm-like Hfq protein increases OxyS RNA interaction with target mRNAs. Mol. Cell **9:**11–22.
36. **Zhang, A., K. M. Wassarman, C. Rosenow, B. C. Tjaden, G. Storz, and S. Gottesman.** 2003. Global analysis of small RNA and mRNA targets of Hfq. Mol. Microbiol. **50:**1111–1124.